Research Square

Preprints are preliminary reports that have not undergone peer review.
They should not be considered conclusive, used to inform clinical practice,
or referenced by the media as validated information.

Ferric citrate and Arsenic Trioxide: A Potent Duo Against Neuroblastoma Through Ferroptosis Activation

Zhixuan Wang
Sun Yat-Sen Memorial Hospital, Sun Yat-Sen University
Yuhan Ma
Sun Yat-Sen Memorial Hospital, Sun Yat-Sen University
Wenxia Wang
Sun Yat-Sen Memorial Hospital, Sun Yat-Sen University
Xiaomin Peng
Sun Yat-Sen Memorial Hospital, Sun Yat-Sen University
Xilin Xiong
Sun Yat-Sen Memorial Hospital, Sun Yat-Sen University
Wenjun Weng
Sun Yat-Sen Memorial Hospital, Sun Yat-Sen University
Yang Li
drliyang@126.com
Sun Yat-Sen Memorial Hospital, Sun Yat-Sen University

Article

Keywords: neuroblastoma, arsenic trioxide, ferroptosis, ferric citrate, iron

Posted Date: February 26th, 2026

DOI: https://doi.org/10.21203/rs.3.rs-8508120/v1

License: This work is licensed under a Creative Commons Attribution 4.0 International License.
Read Full License

Additional Declarations: No competing interests reported.

Abstract

Background

Iron exhibits a close association with neuroblastoma (NB), as elevated serum ferritin is frequently observed in high-risk NB and correlates with an unfavorable prognosis. Ferroptosis, a recently identified cell death modality characterized by iron-dependent lipid peroxidation, involves the crucial triggering role of intracellular free iron overload.

Methods

In this study, we assessed the cellular activity, cellular morphology and reactive oxygen species (ROS) levels in response to ferric citrate (FAC), ATO, and their combination in NB cell lines SK-N-AS and SH-SY5Y. Subsequently, a rescue assay was employed to confirm that the primary mode of NB cell death induced by ATO in conjunction with FAC was ferroptosis.

Results

FAC augmented the inhibitory effects of ATO on NB cells. Increasing FAC concentrations did not significantly promote the proliferation of SK-N-AS and SH-SY5Y NB cell lines. The inhibitory impact of ATO on the proliferation of these NB cell lines was more pronounced with elevated ferroptosis indicators, ROS, in combination with FAC. Moreover, treatment with the ferroptosis inhibitor Fer-1 alleviated the inhibitory effects of ATO in combination with FAC on the two NB cell lines.

Conclusion

Our findings suggest that FAC does not notably contribute to tumor growth but enhances the inhibitory effects of ATO on NB cells. This indicates the potential of FAC combined with ATO as a treatment strategy for NB.

Introduction

Neuroblastoma (NB) is the most common extracranial solid tumor of embryonic origin in childhood [1]. While the overall survival (OS) rate for low- and intermediate-risk NB has surpassed 90%, high-risk NB (HR-NB), comprising approximately half of all NB cases, continues to present clinical challenges [2]. HR-NB is characterized by a propensity for early distant metastasis and a high degree of malignancy, as evidenced by a chemotherapy-induced complete remission rate of only 45% and a 5-year survival rate of less than 15% [3, 4]. Additionally, the development of multidrug resistance (MDR) in advanced stages of HR-NB restricts treatment options and contributes to a high 2-year recurrence rate of 80% [5].

Consequently, pediatric oncologists are compelled by a pressing imperative to investigate economically sustainable and efficacious methodologies for the management of HR-NB.

Iron plays a crucial role in fostering cellular metabolism, proliferation, and growth. Nevertheless, the biological characteristics of malignant tumors frequently involve an imbalance in iron homeostasis and the aberrant activation of iron-regulated genes [6]. Excessive iron loading further stimulates the proliferation, invasion, and distant metastasis of tumor cells [7]. Notably, children diagnosed with HR-NB at the initial stage often exhibit elevated serum ferritin levels, which are correlated with an unfavorable prognosis [8]. However, it is noteworthy that the extent of iron loading within tumor cells can also hold therapeutic potential. Ferroptosis, introduced as a non-apoptotic mode of cell demise by Stockwell's research group in 2012, is initiated through iron-dependent lipid peroxidation [9]. The escalation of intracellular free iron levels precipitates the generation of reactive oxygen species (ROS) free radicals, provoking lipid peroxidation, and ultimately culminating in cell death [10]. The primary recognized mechanisms for triggering ferroptosis involve the GSH-GPX4 pathway and iron overload [9]. Within the iron overload pathway, ferritin degradation through iron autophagy releases stored ferric ions, while heme oxygenase-1 (HO-1) catalyzes heme, leading to the production of ferric ions, thereby inducing intracellular iron overload. This process plays a pivotal role in regulating the activation of ferroptosis [11]. The investigation revealed that inducers of ferroptosis play a pivotal role in the induction of cell death in NB [6, 12]. For instance, Erastin was observed to downregulate the expression of both mRNA and protein associated with Ferroportin1, an iron-transporting protein, within the SH-SY5Y cell line of NB, which resulted in a reduced efflux of iron ions from SH-SY5Y cells, leading to an increased intracellular iron load and subsequent initiation of ferroptotic cell death in NB cells [6]. Synthetic iron complexes, functioning as ferroptosis inducers, hastened the demise of NB1 cells and heightened the cytotoxic impact of the chemotherapeutic drug cisplatin on NB1 cells [12]. These findings propose a prospective strategy for addressing HR-NB. Nevertheless, various small-molecule ferroptosis inducers, such as Erastin and BSO (glutathione synthesis inhibitors), along with RSL3 (a GPX4 inhibitor), are presently in the preclinical phase, with uncertainties surrounding their clinical implementation [13, 14].

Arsenic trioxide (ATO) has a rich history spanning over 2,000 years as a traditional Chinese medicine. Currently, it holds approval for treating acute promyelocytic leukemia and advanced primary hepatocellular carcinoma [15, 16]. In recent years, it has been revealed that the cytotoxic effects of ATO are intricately linked to its distinctive oxidative damage mechanisms. ATO diminishes cellular antioxidant capacity by elevating catalase, malondialdehyde, and ROS levels while concurrently reducing the content of reduced glutathione (GSH) [17]. Moreover, the induction of excessive ROS production by ATO results in the down-regulation of Bcl-2 expression, activation of caspases, disruption of mitochondrial membrane potential, and initiation of structural alterations in DNA, encompassing base mutations, translocations, deletions, sister chromatid exchanges, as well as DNA methylation or demethylation. These processes collectively contribute to the promotion of apoptosis in tumor cells [18, 19]. ATO exhibits anti-tumor effects on NB, as evidenced by our prior investigations, which have elucidated that ATO induces NB cell death through three pathways: apoptosis [20], down-regulation of glycoprotein P [21], and inhibition of the Hedgehog pathway [22]. Moreover, ATO has demonstrated clinical efficacy, enhancing objective

remission rates when combined with conventional chemotherapy [23, 24]. In order to elucidate and enhance the understanding of the anti-tumor mechanism of arsenic trioxide (ATO) on neuroblastoma (NB), we identified differentially expressed proteins enriched in the ferroptosis pathway through proteomics technology, following ATO treatment of the NB cell line SK-N-BE(2) [25]. Our subsequent in vitro experiments demonstrated that ATO induces ferroptosis in NB cells by down-regulating the ferroptosis rate-limiting enzyme, GPX4 [26].

In summary, iron loading exerts a dual influence on NB cells. Elevated iron levels serve as a pivotal prerequisite for the growth of NB tumor cells, enhancing both their proliferative and invasive capabilities. Concurrently, heightened iron concentrations induce the generation of ROS in NB, increasing their susceptibility to ferroptosis. In this study, we undertook the initial endeavor to augment intracellular iron levels in NB cells. Specifically, ferric citrate (FAC) served as a supplementary iron agent in conjunction with ATO, an inducer of ferroptosis, to investigate the potential of this combination in promoting ferroptosis in NB cells.

Materials and methods

Cell Culture

Human SK-N-AS, SH-SY5Y cells were purchased from Asbio Technology (Guangzhou, China). Cells were cultured in DMEM/F12 medium (1:1; Hyclone; GE Healthcare Life Sciences, Logan, UT, USA) supplemented with 10% heat-inactivated fetal bovine serum, at 37°C in an incubator with 5% CO_2. After reaching 80% confluency in a monolayer and multilayers, the cells were transferred to 96-well plates at 1×10^4 cells per well.

Cytotoxicity Assays

Cell Counting Kit 8 (CCK-8) (K1018, Apexbio, USA) was used to measure the cell growth inhibition. The logarithmic cells were inoculated in 96-well with (1–2)×10^4 per well in 100 μl medium. After 12 h of adherent growth, each cell line was treated with ATO (Harbin Yida Pharmaceutical Co., Ltd., Heilongjiang, China) at a concentration gradient. NB cells were treated with serial dilutions of ATO for 24 h. Then, cells were transferred into DMEM medium containing CCK-8 solution at 37℃ for 3 h. The enzyme-linked immunosorbent assay microplate reader (Molecular Devices LLC, Sunnyvale, CA, USA) was used to access the absorbance values at 450 nm. The IC_{50} values of NB cells were calculated using GraphPad Prism version 9.0.

Experimental Groups

Half-maximal inhibitory concentration (IC_{50}) values reflect the killing capacity of the drug. In general, drugs with lower IC_{50} values are more potent [27]. To explore the influence of ATO, FAC, and their

combination on the cell cycle and ROS levels, SK-N-AS, SH-SY5Y cells were divided into three treatment groups and respectively treated for 24 hours with the IC50 of ATO, FAC, and their combination. Controls were medium samples devoid of ATO and FAC.

Cell Morphology

SK-N-AS, SH-SY5Y cells in logarithmic growth phase were inoculated in six-well plates and counted by cell counting plate, about (4 ~ 6)×10^5 cells per well, and blank control group, ATO single drug group, FAC single drug group and ATO combined with FAC group were set up, and the morphology of the cells was observed under the inverted phase contrast microscope after incubation for 24h, and the experiment was repeated three times.

Reactive oxygen species assays

Flow cytometry (FCM) (BD Biosciences, USA) and a ROS assay kit (Beyotime, Shanghai, China) were employed to assess the level of ROS in NB cells. The cells were seeded in 6-well plates with 3 ml of DMEM medium at a density of 8×105 cells overnight and treated with various dilutions of ATO for 12 h. Subsequently, the cells were transferred to serum-free medium containing the fluorescent probe DCFH-DA (1:10000) and incubated in the dark at 37℃ for 20 min. Afterward, the cells were washed three times with phosphate-buffered solution. The green fluorescence intensity was quantified using an automated fluorescent microplate reader (Scientific Varioskan LUX, Thermo Fisher Scientific).

Ferroptosis rescue experiment analysis

Ferroptosis rescue experiment analysis was performed by CCK-8. Following an overnight culture of NB cells, they were subjected to pre-treatment with specific compounds including Deferoxamine (DFO, 100 μM), Ferrostatin-1 (Fer-1, 1 μM), Z-VAD (OH)-FMK (Z-VAD, 10 μM), and Necrostatin-1 (Nec-1, 10 μM) for 1 h. Subsequently, the cells were were treated with ATO at a concentration of 20 μM for 24 h. Subsequently, the cells were evaluated in accordance with the manufacturer's instructions. The absorbance values at 450 nm were measured using an enzyme-linked immunosorbent assay microplate reader.

Statistical Analysis

Each test was performed in triplicate and three times at least. The data was analyzed by GraphPad Prism 9.0 (GraphPad Software, CA, USA). Statistical data are presented as mean ± standard deviation (SD). Normality and variance homogeneity were assessed using the Levene test and Kolmogorov-Smirnov test separately. If the quantitative data met the above conditions, Student’s t-test was used. If the conditions were not met, the rank-sum test was used. $P < 0.05$ was considered statistically significant.

Results

Influence of Different Concentrations of FAC and ATO on the Viability of SK-N-AS and SH-SY5Y Cells

This study established concentration gradients for ATO at 0μM, 3μM, 6μM, 10μM, 12μM, 15μM, 20μM, 40μM, 50μM, 100μM (SK-N-AS cells) and 0μM, 6μM, 8μM, 9μM, 10μM, 11μM, 12μM, 15μM, 20μM, 25μM, 50μM, 100μM (SH-SY5Y cells). Additionally, FAC concentration gradients were set at 0μM, 100μM, 200μM, 300μM, 400μM, 500μM, 600μM, 700μM, 800μM, 900μM, 1mM. Subsequently, SK-N-AS and SH-SY5Y cells were treated with varying concentrations of ATO or FAC, and cell viability was assessed after 24 hours. The results (Figs. 1 and 2) indicate that ATO induces cell death in both SK-N-AS and SH-SY5Y cells, with a more pronounced effect at higher concentrations. Low-dose FAC (5μM and 10μM) promotes NB cell growth, and with increasing FAC concentration, the decrease in NB cell proliferative activity is moderate, not falling below 75%. After 24 hours of ATO treatment, SK-N-AS cell viability across the 3-100 μM concentration gradient was (105.57 ± 8.4)%, (100.26 ± 5.88)%, (92.69 ± 4.8)%, (89.5 ± 5.05)%, (84.41 ± 4.07)%, (81.6 ± 3.8)%, (57.48 ± 1.6)%, (46.55 ± 3.51)%, (21.35 ± 13.69)%, with GraphPad Prism 9.0 calculating IC_{50}ATO = 46.52 μM. For SH-SY5Y cells, viability across the 6μM–100μM concentration gradient was (112.45 ± 1.43)%, (89.87 ± 2.4)%, (65.98 ± 3.11)%, (50.62 ± 3.94)%, (39.3 ± 4.57)%, (28.65 ± 8.18)%, (12.48 ± 7.03)%, (6.39 ± 29.08)%, (5.96 ± 26.2)%, (5.41 ± 36.47)%, (6.59 ± 29.24)%, with GraphPad Prism 9.0 calculating IC_{50}ATO = 10.29 μM. FAC treatment at varying concentrations for SK-N-AS and SH-SY5Y cells after 24 hours yielded viability rates of (105.18 ± 0.32)%, (105.07 ± 0.1)%, (101.64 ± 0.23)%, (98.63 ± 0.09)%, (93.46 ± 0.4)%, (90.72 ± 0.02)%, (89.19 ± 0.73)%, (88.17 ± 0.08%) and (107.59 ± 1.54)%, (102.62 ± 0.7)%, (93.89 ± 1.72)%, (90.11 ± 0.38)%, (85.86 ± 1.46)%, (81.49 ± 0.56)%, (79.87 ± 1.31)%, (76.62 ± 0.41%), respectively.

Impact of Different Concentrations of FAC Combined with ATO on the Growth Inhibition of SK-N-AS and SH-SY5Y Cells

Building upon preliminary findings, this study set ATO concentration gradients at 0μM, 10μM, 20μM, 30μM, 40μM, 50μM, 60μM, 70μM, 80μM, 90μM, 100μM. SK-N-AS and SH-SY5Y cells were treated with varying concentrations of FAC combined with ATO, and cell proliferation inhibition rates were measured 24 h later. The results (Fig. 3) reveal that both ATO monotherapy and combination with FAC induce cell death in SK-N-AS and SH-SY5Y cells. As the ATO concentration increases, the cytotoxic effect becomes more pronounced when FAC concentration remains constant. For the same cell line, with increasing FAC concentration, the IC_{50} ATO decreases. At 50μM, 100μM, and 200μM FAC, the IC_{50}ATO for SK-N-AS and SH-SY5Y cells were 28.18μM, 23.21μM, 16.02μM, and 10.2μM, 9.84μM, 6.87μM respectively.

Influence of Different Drug Combinations on the Morphology of SK-N-AS and SH-SY5Y Cells After 24 Hours

The experiment included a blank control group, ATO monotherapy group, 1mM FAC monotherapy group, and ATO combined with FAC group. After 24 hours, changes in cell morphology were observed through inverted phase-contrast microscopy (Fig. 4). In both cell lines, the ATO monotherapy group exhibited

significant inhibition of cell growth and cell shrinkage compared to the control group. The combined ATO with FAC group showed a more pronounced effect, while the FAC monotherapy group showed no significant changes.

Impact of Different Drug Combinations on the Generation of ROS in SK-N-AS and SH-SY5Y Cells After 24 Hours

The experiment included a blank control group, ATO monotherapy group, FAC monotherapy group, and ATO combined with FAC group. After 24 hours, FCM analysis was used to detect the effect of these treatments on ROS production in SK-N-AS and SH-SY5Y cells. The results (Fig. 5) show that after 24 hours, the ROS levels in SK-N-AS cells for the blank control group, ATO monotherapy group, FAC monotherapy group, and ATO combined with FAC group were (2.02 ± 0.45)%, (17.01 ± 9.21)%, (13.15 ± 0.63)%, (44.71 ± 7.45)%, respectively. In SH-SY5Y cells, the ROS levels were (2.02 ± 0.45)%, (17.01 ± 9.21)%, (13.15 ± 0.63)%, (44.71 ± 7.45)%, respectively. The ATO monotherapy group, FAC monotherapy group, and ATO combined with FAC group exhibited higher ROS levels than the blank control group ($P < 0.05$), and the combined effect of the two drugs was stronger than each drug alone ($P < 0.05$). This suggests that the ATO monotherapy group and FAC monotherapy group induced higher ROS levels than the control group, and the combined effect of the two drugs was stronger than each drug alone.

Impact of Different Cell Death Inhibitors on the Proliferative Activity of SK-N-AS and SH-SY5Y Cells After 24 Hours of Combined ATO and FAC Treatment

The experiment included a blank control group, ATO combined with FAC group, ATO combined with FAC + Fer-1 group, ATO combined with FAC + Z-VAD group, and ATO combined with FAC + Nec-1 group. After 24 hours, the analysis was conducted to detect the proliferative activity of SK-N-AS and SH-SY5Y cells. The results (Fig. 6) show that in both cell lines, the cell proliferation rate of all drug-treated groups significantly decreased compared to the blank control group ($P < 0.05$). Among them, the NB cell proliferation rate of ATO combined with FAC + Fer-1 group, with ferroptosis inhibitor Fer-1 added, was significantly higher than that of all other groups except the blank control group ($P < 0.05$). There was no difference in the NB cell proliferation rate between the other groups ($P > 0.05$) compared to the blank control group. Compared to the blank control group, the cell viability of all treatment groups significantly decreased ($P < 0.05$). In both cell lines, the ATO combined with FAC + Fer-1 group had a significantly higher cell viability than the ATO + FAC group ($P < 0.05$), suggesting that Fer-1 could partially counteract the NB cell-killing effect induced by ATO combined with FAC. Additionally, in the SK-N-AS cell line, there was no statistically significant difference between the ATO combined FAC + Z-VAD group, ATO combined FAC + Nec-1 group, and ATO combined FAC group ($P > 0.05$). Similar results were found in the SH-SY5Y cell line.

Discussion

While a high iron load is imperative for the proliferation of NB tumor cells, attempts to impede their growth through iron chelation or deprivation have proven ineffective [28]. Based on previous research

demonstrating that FAC effectively elevates the labile iron pool (LIP) in cancer cells to induce ferroptosis [29], and our prior findings confirming that ATO monotherapy predominantly triggers ferroptosis rather than other cell death modalities in NB cells [26], we hypothesized that leveraging the inherent high iron susceptibility of NB cells could amplify ferroptotic effects. The accumulation of intracellular redox-active iron represents a critical prerequisite for ferroptosis initiation. This mechanistic rationale motivated our investigation into the synergistic potential of ATO combined with FAC to exacerbate ferroptosis in NB cells.Prior to investigating whether FAC supplementation can potentiate the ferroptosis effect in NB cells, it is imperative to clarify the primary query of whether iron supplementation augments the growth of NB tumor cells and to what extent. Our experimental results did not reveal a significant growth-promoting effect of FAC supplementation on NB cell lines. Low doses of FAC (5μM and 10μM) only marginally promoted the growth of the two NB cell lines, and as the FAC concentration increased, the proliferative activity of NB cells diminished. Therefore, promoting the ferroptosis effect of NB cells through iron supplementation appears feasible. We posit that the observed phenomenon stems from the predominant regulation of iron metabolism in tumor cells by iron regulatory proteins (IRP) 1 and IRP2 [30, 31]. These proteins fulfill crucial roles in intracellular iron storage, release, and the post-transcriptional regulation of genes associated with iron homeostasis. Upon achieving iron homeostasis in the presence of elevated iron levels, a balance is struck between the supply and demand of iron within tumor cells. Even in the event of a subsequent increase in intracellular iron loading, it may not exert further promotion of tumor cell proliferation. Surprisingly, excess iron might impede tumor growth by inducing oxidative damage [32, 33]. Upon ascertaining that FAC does not appreciably enhance the proliferation of NB cell lines, subsequent investigations unveiled a synergistic effect when FAC is combined with the ferroptosis inducer ATO, augmenting iron-induced cell death specifically in SK-N-AS and SH-SY5Y. This substantiates our hypothesis that supplementation with FAC enhances ATO-induced ferroptosis by fostering iron overload in tumor cells. Simultaneously, various cell death inhibitors, namely Fer-1 (a ferroptosis inhibitor), Z-VAD-FMK (an apoptosis inhibitor), and Nec-1 (a necrotic apoptosis inhibitor), were employed to assess the extent of ferroptotic effects in the cytotoxicity of NB cells induced by the combination of ATO with FAC. Our investigation revealed a prevalence of ferroptotic effects, surpassing apoptosis and necrosis, in the ATO and FAC-induced cytotoxicity against SH-SY5Y. Intriguingly, in the SK-N-AS cell line, necrotic effects predominated over ferroptosis. We posit that the signaling cascades governing apoptosis, necrosis, and pyroptosis are intricately interconnected, constituting a multifaceted network of programmed cell death mechanisms [34]. It is plausible that the necrotic apoptosis inhibitor Nec-1 targets the antagonizing receptor-interacting protein kinase 1, serving as feedback within this network, thereby amplifying the necrotic effect and reinforcing the cell-killing efficacy [34]. Additionally, disparities in genetic makeup and cellular status between SK-N-AS and SH-SY5Y, coupled with their distinct sensitivities to ferroptosis, could account for the observed experimental discrepancies relative to expectations.

In terms of feasibility and safety within clinical practice, iron supplementation emerges as a routine treatment measure, benefiting from drug accessibility and high patient compliance. Characterized by a broad spectrum of drug safety thresholds, minimal complications, and unexplored risks, along with a low

likelihood of conflicting with conventional chemotherapy, this treatment option can be readily generalized and applied. Moreover, the capacity for timely intervention with iron removal agents in the face of adverse reactions adds to its overall safety profile. Our preliminary study constitutes the inaugural validation of the potential and efficacy of coadministering iron with ATO to enhance ferroptosis in the treatment of NB. This study serves as an experimental foundation for the development and formulation of a clinical strategy for pharmacological ATO treatment in HR-NB, holding significant clinical implications for improving the overall survival rate among children with HR-NB.

Conclusion

In conclusion, our results suggest that that FAC alone does not exert a significant impact on tumor growth. Nevertheless, it exhibits a synergistic effect in enhancing ATO's inhibitory activity against NB cells. The experimental evidence put forth in this study substantiates the therapeutic potential of ATO and FAC in NB treatment.

Abbreviations

Neuroblastoma NB

overall survival OS

high risk neuroblastoma HR-NB

multidrug resistance MDR

reactive oxygen species ROS

heme oxygenase 1 HO-1

arsenic trioxide ATO

Glutathione GSH

ferric citrate FAC

Flow cytometry FCM

standard deviation SD

hypoxia inducible factor-1α HIF-1α

iron regulatory protein IRP

Declarations

Funds

This work was supported by the Guangzhou Area Clinical Specialty Technology Program (Grant 2023P-TS39), the Sun Yat-Sen Medical-Industrial Integration Cultivating Program (Grant YXYGRH202202), and Heilongjiang Harbin Yida Pharmaceutical Co. (Grant 7670020013).

Conflicts of Interest

The authors have no conflicts of interest.

Ethics Statement

Not applicable.

Author Contribution

Conceptualization: Yang Li; Methodology: Yuhan Ma, Zhixuan Wang; Writing-original draft: Zhixuan Wang; Writing-review and editing: Yang Li; Data curation: Zhixuan Wang, Yuhan Ma; Formal analysis: Zhixuan Wang,Wenxia Wang; Visualization: Wenxia Wang, Yuhan Ma; Supervision: Wenjun Weng; Validation: Xiaomin Peng; Project administration: Xilin Xiong; Funding acquisition: Yang Li.

Acknowledgments

Not applicable.

Data Availability

The data generated in this study are available from the corresponding author upon request.

References

1. Basta, N. O. et al. Factors associated with recurrence and survival length following relapse in patients with neuroblastoma. *Br. J. Cancer*. **115** (9), 1048–1057 (2016).
2. Peinemann, F., Tushabe, D. A., van Dalen, E. C. & Berthold, F. Rapid COJEC versus standard induction therapies for high-risk neuroblastoma. *Cochrane Database Syst. Rev.* **2015** (5), CD010774 (2015).
3. London, W. B. et al. Historical time to disease progression and progression-free survival in patients with recurrent/refractory neuroblastoma treated in the modern era on Children's Oncology Group early-phase trials. *Cancer* **123** (24), 4914–4923 (2017).

4. Dixon, S. J. et al. rd, Stockwell BR. Ferroptosis: an iron-dependent form of nonapoptotic cell death. *Cell* **149** (5), 1060–1072 (2012).
5. Pastor, E. R. & Mousa, S. A. Current management of neuroblastoma and future direction. *Crit. Rev. Oncol. Hematol.* **138**, 38–43 (2019).
6. Geng, N. et al. Knockdown of ferroportin accelerates erastin-induced ferroptosis in neuroblastoma cells. *Eur. Rev. Med. Pharmacol. Sci.* **22** (12), 3826–3836 (2018).
7. Pfeifhofer-Obermair, C., Tymoszuk, P., Petzer, V., Weiss, G. & Nairz, M. Iron in the Tumor Microenvironment-Connecting the Dots. *Front. Oncol.* **8**, 549 (2018).
8. Jung, M., Mertens, C., Tomat, E. & Brüne, B. Iron as a Central Player and Promising Target in Cancer Progression. *Int. J. Mol. Sci.* **20** (2), 273 (2019).
9. Kagan, V. E. et al. Redox phospholipidomics of enzymatically generated oxygenated phospholipids as specific signals of programmed cell death. *Free Radic Biol. Med.* **147**, 231–241 (2020).
10. Yang, W. S. & Stockwell, B. R. Synthetic lethal screening identifies compounds activating iron-dependent, nonapoptotic cell death in oncogenic-RAS-harboring cancer cells. *Chem. Biol.* **15** (3), 234–245 (2008).
11. Hou, W. et al. Autophagy promotes ferroptosis by degradation of ferritin. *Autophagy* **12** (8), 1425–1428 (2016).
12. Sagasser, J. et al. A New Approach in Cancer Treatment: Discovery of Chlorido[N,N'-disalicylidene-1,2-phenylenediamine]iron(III) Complexes as Ferroptosis Inducers. *J. Med. Chem.* **62** (17), 8053–8061 (2019).
13. Yang, W. S. et al. Regulation of ferroptotic cancer cell death by GPX4. *Cell* **156** (1–2), 317–331 (2014).
14. Xie, Y. et al. Ferroptosis: process and function. *Cell. Death Differ.* **23** (3), 369–379 (2016).
15. Iland, H. J. et al. Australasian Leukaemia and Lymphoma Group. All-trans-retinoic acid, idarubicin, and IV arsenic trioxide as initial therapy in acute promyelocytic leukemia (APML4). *Blood* **120** (8), 1570–1580 (2012).
16. Hu, H. T. et al. Arsenic trioxide intravenous infusion combined with transcatheter arterial chemoembolization for the treatment of hepatocellular carcinoma with pulmonary metastasis: Long-term outcome analysis. *J. Gastroenterol. Hepatol.* **32** (2), 295–300 (2017).
17. Chen, H. et al. Toxic effects of arsenic trioxide on spermatogonia are associated with oxidative stress, mitochondrial dysfunction, autophagy and metabolomic alterations. *Ecotoxicol. Environ. Saf.* **190**, 110063 (2020).
18. You, B. R. & Park, W. H. Arsenic trioxide induces human pulmonary fibroblast cell death via increasing ROS levels and GSH depletion. *Oncol. Rep.* **28** (2), 749–757 (2012).
19. Pettersson, H. M. et al. Arsenic trioxide is highly cytotoxic to small cell lung carcinoma cells. *Mol. Cancer Ther.* **8** (1), 160–170 (2009).

20. Qi, K. et al. Pre-application of arsenic trioxide may potentiate cytotoxic effects of vinorelbine/docetaxel on neuroblastoma SK-N-SH cells. *Biomed. Pharmacother*. **113**, 108665 (2019).
21. Liu, L. et al. Low dose of arsenic trioxide inhibits multidrug resistant-related P-glycoprotein expression in human neuroblastoma cell line. *Int. J. Oncol.* **49** (6), 2319–2330 (2016).
22. Liu, X. et al. Arsenic Trioxide inhibits Activation of Hedgehog Pathway in Human Neuroblastoma Cell Line SK-N-BE(2) Independent of Itraconazole. *Anticancer Agents Med. Chem.* **23** (20), 2217–2224 (2023).
23. Li, C. et al. Excellent Early Outcomes of Combined Chemotherapy With Arsenic Trioxide for Stage 4/M Neuroblastoma in Children: A Multicenter Nonrandomized Controlled Trial. *Oncol. Res.* **28** (7), 791–800 (2021).
24. Li, Y. et al. Improved Outcomes with Induction Chemotherapy Combined with Arsenic Trioxide in Stage 4 Neuroblastoma: A Case Series. *Technol. Cancer Res. Treat.* **20**, 15330338211041454 (2021).
25. Feng, C. et al. Arsenic trioxide increases apoptosis of SK-N-BE (2) cells partially by inducing GPX4-mediated ferroptosis. *Mol. Biol. Rep.* **49** (7), 6573–6580 (2022).
26. Su, M. et al. Arsenic trioxide induces ferroptosis in neuroblastoma by mediating GPX4 transcriptional inhibition. *Clin. Transl Sci.* **17** (1), e13716 (2024).
27. Hassannia, B. et al. Nano-targeted induction of dual ferroptotic mechanisms eradicates high-risk neuroblastoma. *J. Clin. Invest.* **128** (8), 3341–3355 (2018).
28. Lang, J. et al. Targeted Co-delivery of the Iron Chelator Deferoxamine and a HIF1α Inhibitor Impairs Pancreatic Tumor Growth. *ACS Nano*. **13** (2), 2176–2189 (2019).
29. Fang, S., Yu, X., Ding, H., Han, J. & Feng, J. Effects of intracellular iron overload on cell death and identification of potent cell death inhibitors. BIOCHEM BIOPH RES CO. 2018-09-03; 503 (1): 297–303 .
30. Zhihui, G. & Houbao, L. Progress of the relationship between iron metabolism and solid tumors. *Cancer Res. Clin.* **31** (9), 637–640 (2019).
31. Núñez-Millacura, C., Tapia, V., Muñoz, P., Maccioni, R. B. & Núñez, M. T. An oxidative stress-mediated positive-feedback iron uptake loop in neuronal cells. *J. Neurochem*. **82** (2), 240–248 (2002).
32. Chansiw, N., Kulprachakarn, K., Paradee, N., Prommaban, A. & Srichairatanakool, S. Protection of Iron-Induced Oxidative Damage in Neuroblastoma (SH-SY5Y) Cells by Combination of 1-(N-Acetyl-6-aminohexyl)-3-hydroxy-2-methylpyridin-4-one and Green Tea Extract. *Bioinorg. Chem. Appl.* **2021**, 5539666 (2021).
33. Aguirre, P., Valdés, P., Aracena-Parks, P., Tapia, V. & Núñez, M. T. Upregulation of gamma-glutamate-cysteine ligase as part of the long-term adaptation process to iron accumulation in neuronal SH-SY5Y cells. *Am. J. Physiol. Cell. Physiol.* **292** (6), C2197–C2203 (2007).
34. Jorgensen, I., Rayamajhi, M. & Miao, E. A. Programmed cell death as a defence against infection. *Nat. Rev. Immunol.* **17** (3), 151–164 (2017).

Figures

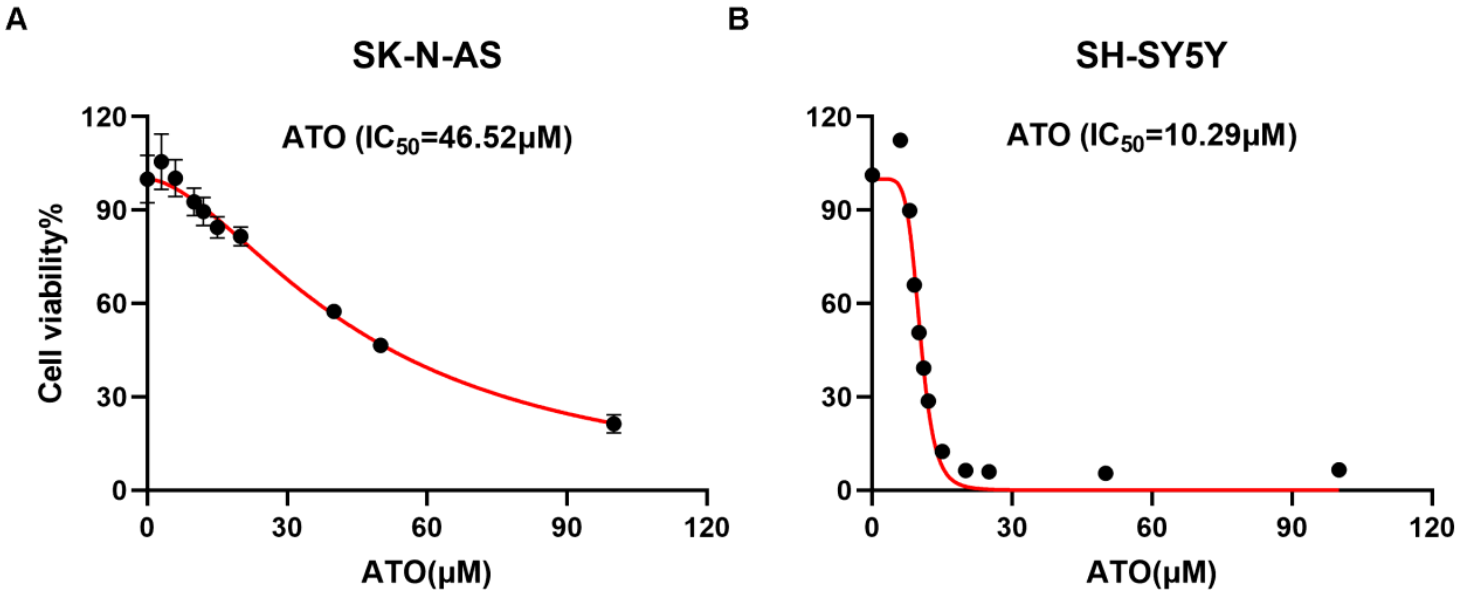


Figure 1

Cell activity rate of **(A)** SK-N-AS and **(B)** SH-SY5Y cells after ATO treatment with different concentrations for 24 h. n=3.

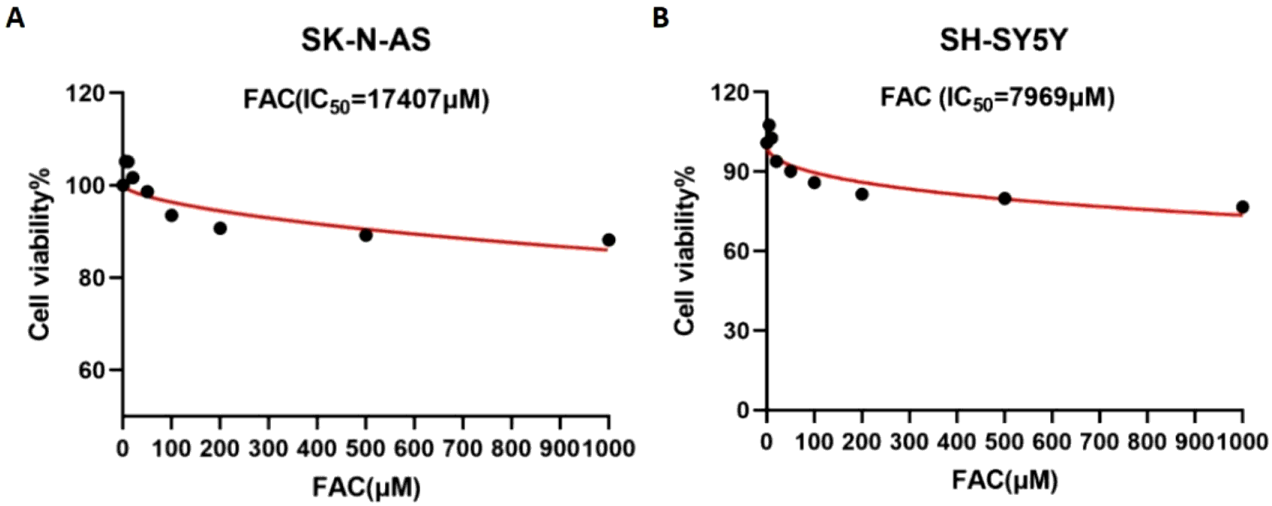


Figure 2

Cell activity rate of **(A)** SK-N-AS and **(B)** SH-SY5Y cells after 24 h treatment with different concentrations of FAC. n=3.

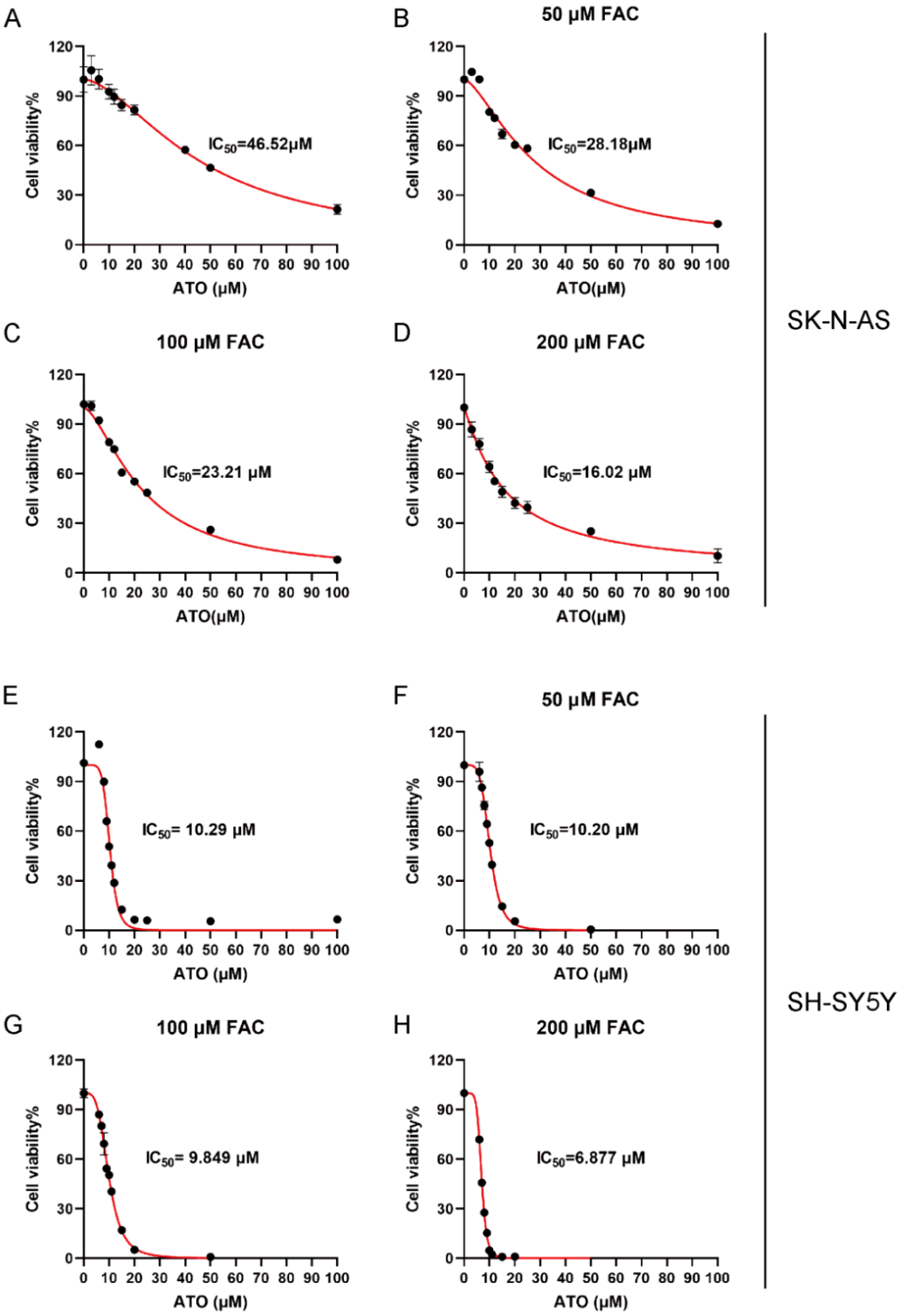


Figure 3

Cell activity rates of SK-N-AS and SH-SY5Y cells were assessed after a 24-h treatment with varying concentrations of FAC in combination with ATO. **(A-D)** In the case of the SK-N-AS cell line, the cell activity rates were examined by introducing a gradient concentration of ATO at specific FAC concentrations (0 μM, 50 μM, 100 μM, and 200 μM, respectively). The IC_{50} values of ATO were determined for the SK-N-AS cell line at FAC concentrations of 50 μM, 100 μM, and 200 μM, respectively. **(E-H)** For the SH-SY5Y cell

line, the cellular activity rates were investigated by applying gradient concentrations of ATO at specific FAC concentrations (0 μM, 50 μM, 100 μM, and 200 μM, respectively). The respective ATO IC_{50} values for the SH-SY5Y cell line at FAC concentrations of 50 μM, 100 μM, and 200 μM. n=3.

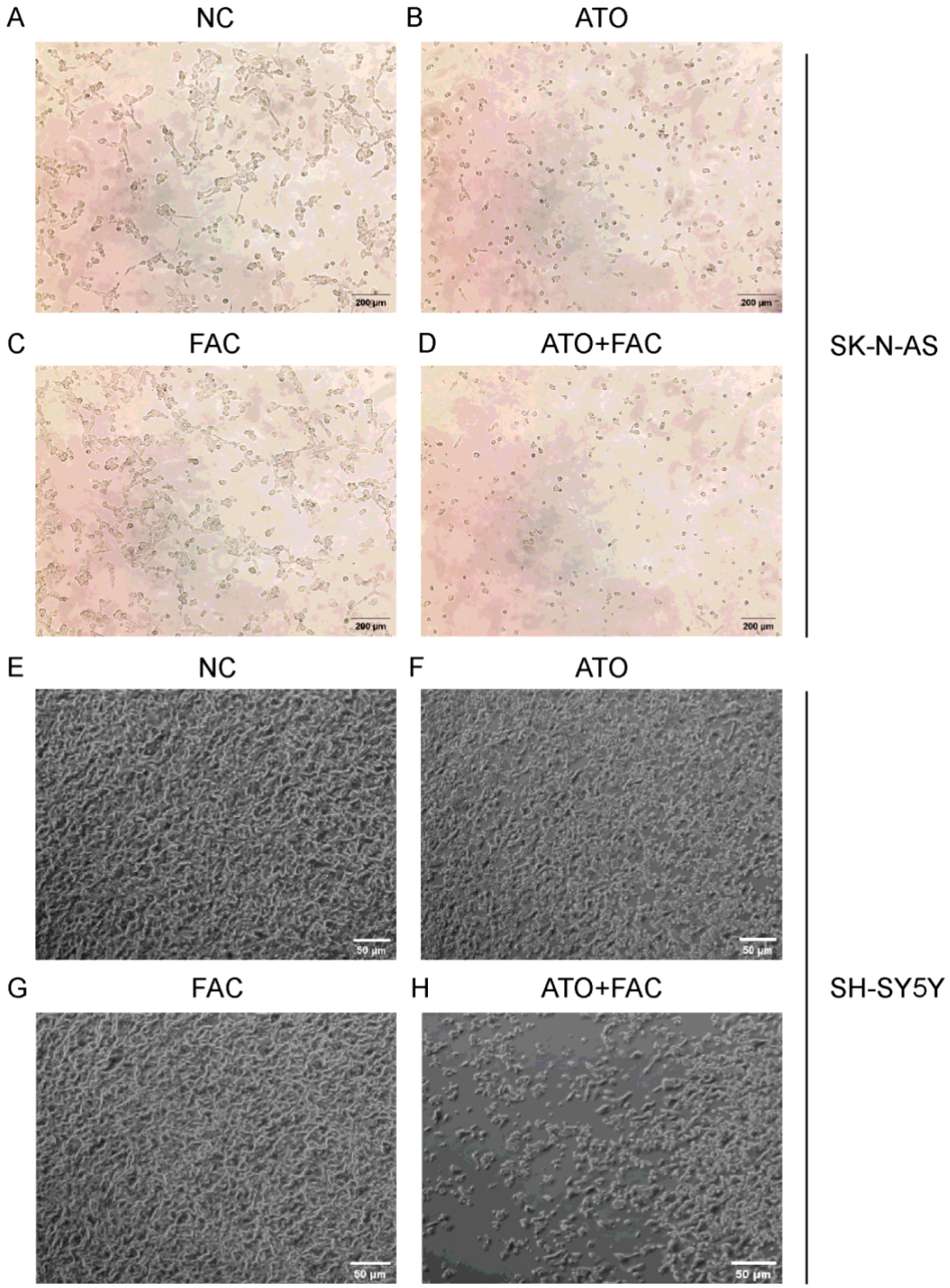


Figure 4

Light microscopy of SK-N-AS and SH-SY5Y cell morphology after 24h treatment with different drug combinations. SK-N-AS (magnification 50×): **(A)** blank control group; **(B)** ATO single-drug group; **(C)**FAC

single-drug group; **(D)** ATO coupled with FAC group.SH-SY5Y (magnification 200×): **(E)** blank control group; **(F)**ATO single-drug group; **(G)** FAC single-drug group; **(H)** ATO coupled with FAC group. n=3.

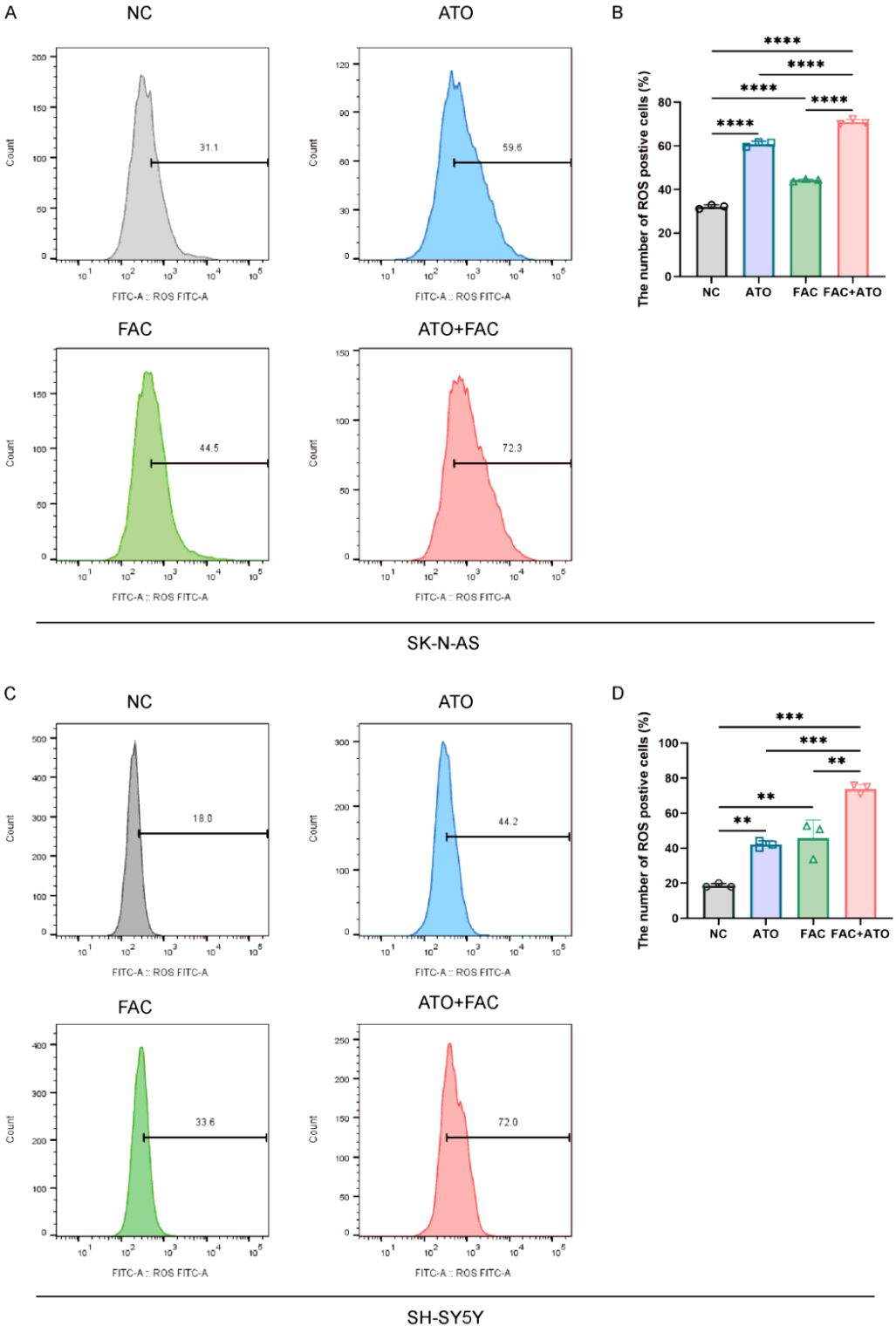


Figure 5

The combination of FAC and ATO facilitated the increase in ROS levels and induced ferroptosis in NB cells. NB cells were treated with 10 μM ATO, 100 μM FAC, and a combination of 10 μM ATO and 100 μM FAC for 12 hours. Subsequently, lipid ROS levels were assessed using FCM with DCFH-DA 581/591

fluorescence staining. Panels **(A-B)** represent the results for SK-N-AS cells, while panels **(C-D)** correspond to SH-SY5Y cells. n=3; ** P<0.01; *** P<0.001; **** P<0.0001.

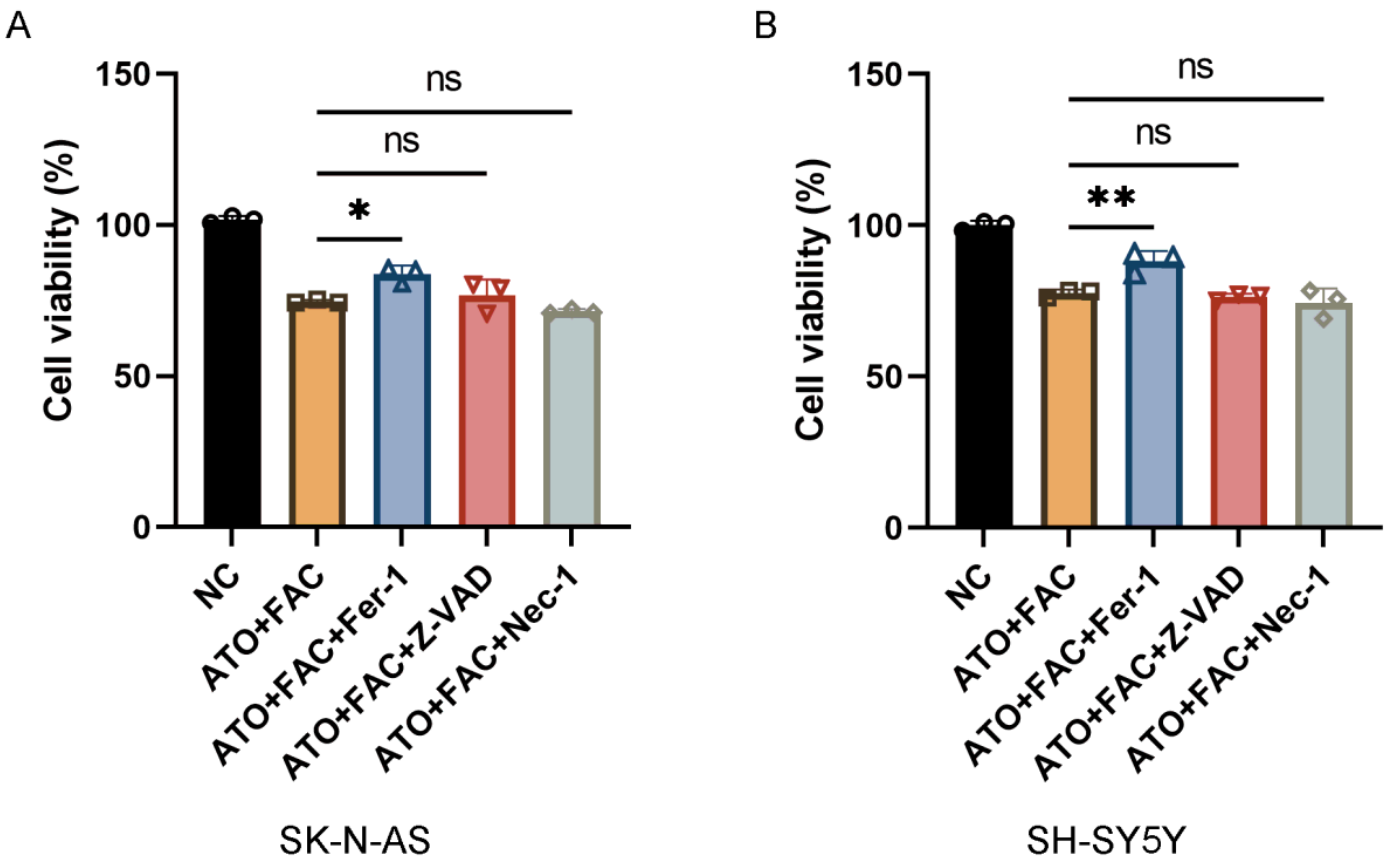


Figure 6

The cell viability rates of **(A)** SK-N-AS and **(B)** SH-SY5Y cells were evaluated following a 24-h treatment with a combination of FAC and ATO, along with various cell death inhibitors. n=3; ns, no significance; * P<0.05; ** P<0.01.